Child abuse associates with increased recruitment of perineuronal nets in the ventromedial prefrontal cortex: possible implication of oligodendrocyte progenitor cells

Arnaud Tanti[1,4], Claudia Belliveau[1,2], Corina Nagy[1], Malosree Maitra[1,2], Fanny Denux[1], Kelly Perlman[1,2], Frank Chen[1], Refilwe Mpai[1,2], Candice Canonne[1], Maria Antonietta Davoli[1], Gustavo Turecki[1,2,3] and Naguib Mechawar[1,2,3]

Affiliations:

[1] McGill Group for Suicide Studies, Douglas Mental Health University Institute, McGill University, Montreal, QC, Canada

[2] Integrated Program in Neuroscience, McGill University, Montreal, QC, Canada

[3] Department of Psychiatry, McGill University, Montréal, QC, Canada

[4] current affiliation : INSERM UMR1253, Tours, France

Corresponding authors:

Naguib Mechawar, PhD
McGill Group for Suicide Studies
Douglas Mental Health Institute
Department of Psychiatry
McGill University
naguib.mechawar@mcgill.ca

Arnaud Tanti, PhD
INSERM UMR1253
arnaud.tanti@univ-tours.fr

Abstract

Child abuse (CA) is a strong predictor of psychopathologies and suicide, altering normal trajectories of brain development in areas closely linked to emotional responses such as the prefrontal cortex (PFC). Yet, the cellular underpinnings of these enduring effects are unclear. Childhood and adolescence are marked by the protracted formation of perineuronal nets (PNNs), which orchestrate the closure of developmental windows of cortical plasticity by regulating the functional integration of parvalbumin interneurons (PV) into neuronal circuits. Using well-characterized post-mortem brain samples, we show that a history of CA is specifically associated with increased recruitment and maturation of PNNs in the ventromedial PFC. Through single-nucleus sequencing and fluorescent in-situ hybridization, we found that the expression of canonical components of PNNs is highly enriched in oligodendrocyte progenitor cells (OPCs), and that they are upregulated in CA victims. These findings suggest that early-life adversity may lead to persistent patterns of maladaptive behaviors by reducing the neuroplasticity of cortical circuits through the enhancement of developmental OPC-mediated PNN formation.

Introduction

Child abuse (CA) has enduring effects on psychological development. Severe adversity during sensitive periods, during which personality traits, attachment patterns, cognitive functions and emotional responses are shaped by environmental experiences, has a profound effect on the structural and functional organization of the brain [1].

At the cellular level, childhood and adolescence are marked by the protracted maturation of neural circuits, characterized by windows of heightened plasticity that precede the development of functional inhibitory connections and the balance of excitatory-inhibitory neurotransmission [2]. A major mechanism involved in this process is the recruitment of perineuronal nets (PNNs), a condensed form of extracellular matrix forming most notably around parvalbumin-expressing (PV+) interneurons. PNNs are thought to gradually decrease heightened plasticity by stabilizing the integration and function of PV+ cells into cortical networks and hindering the remodeling of these networks [3,4]. This has been notably linked to the persistence of long-term associations, including fear memories [5–7].

Evidence in rodents suggests that early-life stress associates with precocious functional maturation of PV+ neurons and the early emergence of adult-like characteristics of fear and extinction learning [8], in addition to discrete changes in the immunoreactivity of inhibitory neuron markers and PNNs [9]. Taken together, these observations suggest that CA may alter the formation of PNNs.

We addressed this question using well-characterized post-mortem samples (Douglas-Bell Canada Brain Bank) from adult depressed suicides who died during an episode of major depression with (DS-CA) or without (DS) a history of severe CA and from matched psychiatrically healthy individuals (CTRL). Standardized psychological autopsies were conducted to provide comprehensive post-mortem diagnostic and retrieve various dimensions of childhood experience, including history and severity of CA. We focused on the ventromedial prefrontal cortex (vmPFC), a brain area closely linked to emotional learning and which is structurally and functionally altered in individuals with a history of CA [1].

Materials and Methods

Human post-mortem brain samples. Brain samples were obtained from the Douglas-Bell Canada Brain Bank (Montreal, Canada). Phenotypic information was retrieved through standardized psychological autopsies, in collaboration with the Quebec Coroner's Office and with informed consent from next of kin. Presence of any or suspected neurological/neurodegenerative disorder signaled in clinical files constituted an exclusion criterion. Cases and controls are defined with the support of medical charts and Coroner records. Proxy-based interviews with one or more informants best acquainted with the deceased are supplemented with information from archival material obtained from hospitals, Coroner's office and social services. Clinical vignettes are then produced and assessed by a panel of clinicians to generate DSM-IV diagnostic criteria, providing sociodemographic characteristics, social developmental history, DSM-IV axis I diagnostic information and behavioural traits; information that is obtained through different adapted questionnaires. Toxicological assessments and medication prescription are also obtained. Presence of severe child abuse was based on adapted Childhood Experience of Care and Abuse (CECA) interviews assessing various dimensions of childhood experience, including abuse (Bifulco et al., 1994). Subjects characteristics are described in **Table 1.**

Tissue dissections

Dissections were performed by expert brain bank staff on fresh-frozen 0.5 cm thick coronal sections with the guidance of a human brain atlas. Ventromedial prefrontal cortex samples were dissected in sections equivalent to plate 3 (approximately − 48 mm from the center of the anterior commissure) of this atlas. Samples were either kept frozen or fixed overnight in 10% formalin until processed for in situ hybridization or immunohistochemistry, respectively.

Immunohistochemistry

Frozen tissue blocks were fixed in 10% neutral buffered formalin overnight at 4 °C, rinsed in PBS and kept in 20% sucrose/PBS solution until serially sectioned at 40 µm on a cryostat. Free-floating sections were rinsed in phosphate-buffered saline (PBS) and then incubated overnight at 4ºC under constant agitation with a mouse anti-NeuN antibody (Millipore, 1:500, MAB377) and biotinylated Wisteria Floribunda Lectin (WFL, Vector Laboratories, B-1355; 1:2500) diluted in a

blocking solution of PBS/0.2% Triton-X/2% normal donkey serum. Sections were then rinsed and incubated for 2h at room temperature with Cy3-conjugated Streptavidin (Jackson ImmunoResearch, 016-160-084; 1:500) for the detection of PNNs and Alexa-488 conjugated anti-Mouse (Jackson ImmunoResearch, 1:500) for NeuN, diluted in the same blocking solution as the primary incubation. Following the secondary antibody incubation, sections were rinsed, endogenous autofluorescence from lipofuscin and cellular debris was quenched with Trueblack (Biotium), and sections were mounted on Superfrost charged slides and coverslipped with Vectashield mounting medium (Vector Laboratories, H-1800).

Whole vmPFC sections were scanned on a Zeiss Axio Imager M2 microscope equipped with a motorized stage and Axiocam MRm camera at x20. The ImageJ software (NIH) Cell Counter plugin was used to manually count PNNs. An average of 4 sections per subject was used. Cortical layers were delineated based on NeuN+ cells distribution and morphology, and the number of PNNs as well as the area of each layer were measured, allowing to generate PNNs density values (n/mm^2).

Fluorescent in situ hybridization

Frozen BA9 blocks were cut serially with a cryostat and 10µm-thick sections collected on Superfrost charged slides. In situ hybridization was performed using Advanced Cell Diagnostics RNAscope® probes and reagents following the manufacturer instructions. Sections were first fixed in cold 10% neutral buffered formalin for 15 minutes, dehydrated by increasing gradient of ethanol bathes and air dried for 5 minutes. Endogenous peroxidase activity was quenched with hydrogen peroxide for 10 minutes followed by protease digestion for 30 min at room temperature. The following probes were then hybridized for 2 hours at 40C in a humidity-controlled oven: Hs-PVALB (cat. no. 422181), Hs-VCAN (cat. no. 430071-C2), Hs-PDGFRA (cat. no. 604481-C3), Hs-TNR (cat. no. 525811), Hs-PTPRZ1 (cat. no. 584781-C2). Amplifiers were added using the proprietary AMP reagents, and the signal visualized through probe-specific HRP-based detection by tyramide signal amplification with Opal dyes (Opal 520, Opal 570 or Opal 690; Perkin Elmer) diluted 1:700. Slides were then coverslipped with Vectashield mounting medium with DAPI for nuclear staining (Vector Laboratories) and kept at 4C until imaging. For immunohistochemical staining of PNNs following PVALB in situ hybridization, slides were

rinsed in PBS, incubated overnight at 4C with biotinylated WFL followed by Cy3-conjugated Streptavidin for 2 hours prior to coverslipping.

Imaging and analysis of in situ RNA expression in OPCs

Image acquisitions was performed on a FV1200 laser scanning confocal microscope (FV1200) equipped with a motorized stage. For each experiment and subject, 6 to 10 stack images were taken to capture at least 20 OPCs (PDGFRA+) per subject. Images were taken using a x60 objective (NA = 1.42) with a XY pixel width of ~0.25µm and Z spacing of 0.5µm. Laser power and detection parameters were kept consistent between subjects for each set of experiment. Since TSA amplification with Opal dyes yields a high signal to noise ratio, parameters were optimized so that autofluorescence from lipofuscin and cellular debris was filtered out. OPCs were defined by bright clustered puncta-like PDGFRA signal present within the nucleus of the cells. Using ImageJ, stacks were first converted to Z-projections, and for each image the nuclei of OPCs were manually contoured based on DAPI expression. Expression of VCAN, TNR or PTPRZ1 in OPCs was quantified using the area fraction, whereby for each probe the signal was first manually thresholded and the fraction of the contoured nucleus area covered by signal measured for each OPC. Area fraction was the preferred measure to reflect RNA expression as punctate labeling generated by FISH often aggregates into clusters that cannot readily be dissociated into single dots or molecules.

Ratios of PVALB+/PNN+ cells

Proportions of PVALB+ cells enwrapped by PNNs were determined in a single section. An average of 55 PVALB+ cells per subject were imaged under a x20 objective through layers 4-5 of the vmPFC.

Intensity and area measurements

For each subject, ~15 z-stacks (0.26µm Z-spacing) spanning all layers of the vmPFC were acquired at 40x magnification on an Olympus FV1200 laser scanning confocal microscope. PNNs were traced manually with ImageJ using maximum intensity projections generated from each stack. For each PNN, the mean pixel value of adjacent background was subtracted to the mean pixel value of the contoured soma of the PNN, yielding the mean corrected fluorescence

intensity. To infer on their morphological complexity, we measured the area covered by each contoured PNN, including soma and ramifications extending over proximal dendrites.

Cell-type specific expression of PNN canonical components using single-nucleus sequencing

Cell-type specific expression of canonical components of PNNs was explored using a snRNA-seq dataset from the human prefrontal cortex previously generated by our group [10], for which methodology is extensively described in this published resource. Average expression for each PNN component in each cell type was calculated by weighting the expression values (normalized transcript counts) of each cluster by the size (number of nuclei) of the cluster. Weighted average expression values are displayed in a heatmap, scaled by row (i.e. gene). The color bar therefore represents the expression values as z-scores, with darker colors indicating higher expression.

Statistical analyses

Analyses were performed on Statistica version 12 (StatSoft) and Prism version 6 (GraphPad Software). Distribution and homogeneity of variances were assessed with Shapiro–Wilk and Levene's tests, respectively. PNNs densities were analyzed using a mixed-effects model, using layer and group as fixed factors, followed by Tukey's HSD test for corrected post hoc comparisons. For all other variables (WFL intensity, WFL area per PNN, PNN+/PVALB ratios, RNA expression in OPCs and distance of OPCs from PVALB+ cells) group effects were detected using one-way ANOVAs or Kruskal-Wallis test followed by Tukey's HSD or Dunn's test respectively. Linear regressions were used to address the relationship between PNNs densities, distance of OPCs from PVALB+ cells, and RNA expression of canonical components of PNNs. Significance threshold was set at 0.05.

Results

PNNs densities, visualized by Wisteria Floribunda Lectin (WFL) labeling and NeuN immunostaining (**Fig.1A**) were markedly higher in the vmPFC of individuals with a history of CA compared to controls and depressed suicides with no history of CA (**Fig.1B)**. To understand whether these changes were directly linked to increased PNNs recruitment rather than changes in PV+ cells numbers, we compared ratios of PV+ cells surrounded by PNNs. PV antigenicity is

particularly susceptible to freezing, and lost altogether in samples snap frozen prior to fixation. We therefore developed an approach to combine fluorescence in-situ hybridization (FISH) and immunofluorescence to visualize PVALB expressing cells and PNNs in frozen samples (**Fig.1C**). ~65% of PVALB+ cells were surrounded by PNNs (**Fig.1D**), in line with previous observations. Importantly, samples from DS-CA individuals displayed a robust increase in the percentage of PVALB+ cells surrounded by PNNs compared to DS and CTRL samples (**Fig.1D)**

To investigate if CA associates with maturational changes of PNNs, we compared the intensity of WFL staining between groups (**Fig.1E**) as an indication of their maturity (10), as well as the area covered by individual PNNs as an indicator of their morphological complexity. CA was both associated with higher intensity of WFL staining per PNN (**Fig.1F**) and cells more extensively covered by PNNs (**Fig.1G**), suggesting overall that CA may precipitate both the maturation and the recruitment of PNNs around PV+ cells.

We then sought to explore the molecular underpinnings of this phenomenon, and reasoned that increased recruitment of PNNs associated with CA should translate or be induced by changes in the molecular programs controlling PNN assembly. Our understanding of these transcriptional programs is scarce, hindered by the fact that several known molecules participating in PNN recruitment are released non-locally and by different cell types, implying a complex cellular crosstalk orchestrating PNN assembly. To gain insight into how, in humans, different cell types contribute to the synthesis of canonical components of PNNs, we explored a single-nucleus sequencing dataset previously generated by our group in the human PFC [10], and screened their expression across 8 major cell types. The main canonical components of PNNs, namely aggrecan, neurocan, versican, phosphacan, brevican, and tenascin-R, were highly enriched in oligodendrocyte progenitor cells (OPCs) (**Fig.2A**). This was further validated using FISH (**Fig.2B and 2C**) for versican (VCAN) and phosphacan (PTPRZ1), as they showed the strongest expression in OPCs and are two major signature genes in late OPCs [11]. We found that virtually all PDGFRA+ OPCs express high levels of these components, while cells expressing these genes are almost all PDGFRA+ OPCs (**Fig.2D and 2E**). This suggests that OPCs are likely potent regulators of PNN formation.

OPCs were on occasions directly juxtaposed to PVALB+ cells (**Fig.2B**), as previously reported in rodents [12]. Interestingly, OPC proximity to PVALB+ cells modestly correlated with PNN density (**Fig.2F**), and was increased in individuals with a history of CA (**Fig.2G**), further suggesting an interplay between these two cell types. In support of a possible involvement of OPCs in mediating CA-related changes in PNNs, the expression of both PTPRZ1 and TNR in OPCs correlated with PNNs densities (**Fig.2H and 2I**) and were upregulated in OPCs of CA victims (**Fig.2J-L**).

Discussion

Overall, our results suggest that a history of CA associates with increased recruitment and maturation of PNNs, as well as an upregulation of their canonical components by OPCs, a cell type that likely plays a key role in the cellular crosstalk that orchestrates PNN formation.

Although, to our knowledge, this is the first evidence in humans that early-life adversity (ELA) affects the recruitment of PNNs, recent studies in animals have approached this question. Guadagno et al.[13] found that in the limited bedding paradigm, adolescent pups have increased densities of PNNs in the amygdala. Murthy and al.[9] showed that in the ventral dentate gyrus, maternal separation combined with early-weaning, another model of early-life stress mimicking some aspects of adversity, led to an increase in PNN intensity around parvalbumin-positive interneurons with no change in PNN density. Importantly, these effects were present in adults, suggesting a long-lasting impact of ELA on PV function and PNN remodeling. Gildawie et al.[14] also recently reported that in the prelimbic cortex, maternal separation in rats increased the intensity of PNNs surrounding PV+ neurons, an effect only observed in adulthood. This suggests that changes in PNN integrity and maturation following ELA could possibly be protracted and develop over time. While we can't address this question with our postmortem design, our results show at the very least that changes in PNN integrity in victims of CA are observable at adult age. Few studies have so far been conducted on this topic, however, with one of them showing a decrease in the intensity of WFA fluorescent labeling in both the prefrontal cortex and hippocampal CA1 following an early-life sub-chronic variable stress paradigm[15]. Clearly, more work is needed to better characterize the effects of ELA on PNNs integrity, particularly in light of the multiple paradigms used in animal studies.

One particularly noteworthy aspect of our results is the specific association between changes in PNNs and a history of CA. Because such changes are absent in depressed suicides without a history of CA, our findings suggest possible vulnerability windows during which PV cell function and PNN maturation are more susceptible to experience-dependent remodeling and adversity. If these changes may mediate some of the negative mental health outcomes or cognitive and emotional traits associated with CA in adulthood, they likely don't represent a hallmark of depression, in accordance with a recent post-mortem study finding no change in the density of PNNs in the PFC of depressed patients[16].

The search for possible mechanisms involved in the effects of ELA on PNNs development is an unexplored field. PNN recruitment is likely orchestrated by a complex interplay between activity-dependent autonomous pathways in parvalbumin neurons, with signals originating from different cell types involved in their assembly. Because parvalbumin neurons have been shown to be particularly sensitive to stress and glucocorticoids, in particular early-life stress[17–22], we can speculate that elevated glucocorticoids in CA victims[23] can impact PV neuron function early-on. This could translate into increased GABA release following GR activation[21], and indirect increase in the recruitment of PNNs, which has been directly linked to PV neuron activity[24,25] and GABA levels[26]. A myriad of factors could however indirectly affect PV cells during this period of protracted maturation associated with childhood and adolescence, such as increased pro-inflammatory cytokine expression associated with ELA[18,27] or changes in neurotrophic factor expression[28–30].

An interesting molecular candidate is the transcription factor OTX2, released non-locally by cells in the choroid plexus, and acting as a major initiator of PNN development[31]. Recent evidence suggests a role of OTX2 in mediating vulnerability to early-life stress[32], and Murthy et al. reported elevated expression of OTX2 in the choroid plexus following maternal separation and around PV+/PNNs+ cells in the ventral dentate gyrus[9]. While the precise mechanisms involved in the effects of ELA on the release of OTX2 are not known, it is noteworthy that DNA methylation of the OTX2 gene in children has been shown to correlate with increased risk for depression as well as increased functional connectivity between the vmPFC and bilateral regions of the medial frontal cortex[33]. This highlights that beyond discrete changes in PV cell function,

ELA could affect the release of distal cues by non-neuronal cells and contribute to extracellular matrix remodeling, thus affecting brain function and vulnerability to psychopathology.

As mentioned previously, although PNN development has been strongly linked to neuronal activity[3,24,34], PNN integrity and assembly are likely orchestrated by the complex integration by PV neurons of cues originating from multiple cell types[35,36]. Accordingly, we found that the expression of genes encoding for the major canonical components of PNNs were strongly enriched in oligodendrocyte-lineage cells, in particular in OPCs, while PV neurons barely expressed any of those components. This is in accordance with previous literature in rats, albeit in the cerebellum, similarly showing that Versican (VCAN), Phosphacan (PTPRZ1) and Tenascin-R (TNR) are almost exclusively expressed in oligodendrocyte-lineage cells[37]. This is also consistent with more recent single-cell RNAseq studies showing an enrichment of extracellular components, including VCAN and PTPRZ1, in OPCs[38–40].

The interplay between oligodendrocyte-lineage cells and PV neurons, in particular during developmental windows of plasticity, are being increasingly documented[41]. Interestingly, OPCs have been shown to be ontogenetically related to PV neurons[42]. OPCs also receive functional synaptic inputs from GABAergic interneurons, a connectivity that reaches its peak during early postnatal development and the maturation of PNNs[43–45]. It is therefore particularly tempting to speculate that OPC-PV neurons communication during critical windows of development may play a fundamental role in modeling cortical plasticity and the maturation of PNNs. This has never been addressed, and we therefore approached this question by investigating how CA associates with changes in the expression of PNN canonical components specifically in OPCs, and how this correlates with the changes in PNN integrity observed in victims of CA. In support of this hypothesis, we found that OPC proximity to PV neurons positively correlated with PNN densities, and that in victims of CA, OPCs tended to be more proximal to PV neurons. We also found that the expression of canonical components of PNNs in OPCs was positively correlated with PNN densities and upregulated in victims of CA. This strongly suggests that CA has a durable impact on OPC molecular programs that may contribute to PNN development. This also further strengthens previous reports by our group[46,47] that CA has profound effects on oligodendrocyte-lineage cells, that may extend well beyond affecting myelination by contributing to the reprogramming of various aspects of brain plasticity.

How precisely OPC-PV communication contributes to the development of PNNs and impacts PV neurons functional integration and circuit dynamics certainly deserves further investigation using more functional approaches. Inherent to our post-mortem design, a major limitation of this study lies in our inability to infer on the precise timing of these changes, and whether dynamic remodeling of the extracellular matrix occurs in a protracted way. Another limitation is that our study only included very few female samples, given the much higher prevalence of suicide in males. Sex is known to moderate both the biological and the psychopathological effects of CA[48], and increasing evidence points towards a sexual dimorphism in the effects of stress, in particular early-life stress, on PV neuron function and perhaps PNN development[8,22,49]. Future studies should therefore explore this aspect to further understand how ELA modifies trajectories of brain development.

In conclusion, our findings suggest that CA may lead to persistent patterns of maladaptive behaviors by reducing the neuroplasticity of cortical circuits through the enhancement of developmental OPC-mediated PNN formation. Future preclinical models should help determine whether changes in OPCs are causal in the increased recruitment of PNNs following CA or an indirect response following altered PNN dynamics. Likewise, the consequences of these molecular changes should be examined at the network level to determine their functional impact on intra- and inter-regional communication.

Acknowledgments and funding

This work was funded by a CIHR Project grant to NM. AT was supported by fellowships from the FRQS and Toronto Dominion, and an American Foundation for Suicide Prevention (AFSP) Young Investigator Innovation Grant (YIG-0-146-17). The Molecular and Cellular Microscopy Platform and the Douglas-Bell Canada Brain Bank (DBCBB) are partly funded by a Healthy Brains for Healthy Lives (CFREF) Platform Grant to GT and NM. The DBCBB is also funded by the Réseau Québécois sur le suicide, le troubles de l'humeur et les troubles associés (FRQS).

Author Contributions

AT and NM conceived the study. GT participated in the acquisition and clinical characterization of the brain samples. AT, CB, FD, MAD, CC, RM contributed to immunohistological

experiments. AT, CN, MM and KP generated and analyzed the snRNA-seq dataset. AT and FC performed the in-situ hybridization experiments. AT and NM prepared the manuscript and all authors contributed to and approved its final version.

Competing Interest Statement: The authors have no financial interest or conflict of interest to declare.

References

1 Teicher MH, Samson J a., Anderson CM, Ohashi K. The effects of childhood maltreatment on brain structure, function and connectivity. *Nat Rev Neurosci* 2016; **17**: 652–666.

2 Ferguson BR, Gao W-J. PV Interneurons: Critical Regulators of E/I Balance for Prefrontal Cortex-Dependent Behavior and Psychiatric Disorders. *Front Neural Circuits* 2018; **12**: 37.

3 Fawcett JW, Oohashi T, Pizzorusso T. The roles of perineuronal nets and the perinodal extracellular matrix in neuronal function. Nat. Rev. Neurosci. 2019. doi:10.1038/s41583-019-0196-3.

4 Sorg BA, Berretta S, Blacktop JM, Fawcett JW, Kitagawa H, Kwok JCF *et al.* Casting a wide net: Role of perineuronal nets in neural plasticity. In: *Journal of Neuroscience*. Society for Neuroscience, 2016, pp 11459–11468.

5 Gogolla N, Caroni P, Lüthi A, Herry C. Perineuronal nets protect fear memories from erasure. *Science (80-)* 2009; **325**: 1258–1261.

6 Thompson EH, Lensjø KK, Wigestrand MB, Malthe-Sørenssen A, Hafting T, Fyhn M. Removal of perineuronal nets disrupts recall of a remote fear memory. *Proc Natl Acad Sci U S A* 2018; **115**: 607–612.

7 Shi W, Wei X, Wang X, Du S, Liu W, Song J *et al.* Perineuronal nets protect long-term memory by limiting activity-dependent inhibition from parvalbumin interneurons. *Proc Natl Acad Sci U S A* 2019. doi:10.1073/pnas.1902680116.

8 Bath K, Manzano-Nieves G, Goodwill H. Early life stress accelerates behavioral and neural maturation of the hippocampus in male mice. *Horm Behav* 2016; **82**: 64–71.

9 Murthy S, Kane GA, Katchur NJ, Lara Mejia PS, Obiofuma G, Buschman TJ *et al.* Perineuronal Nets, Inhibitory Interneurons, and Anxiety-Related Ventral Hippocampal Neuronal Oscillations Are Altered by Early Life Adversity. *Biol Psychiatry* 2019; **85**: 1011–1020.

10 Nagy C, Maitra M, Tanti A, Suderman M, Théroux JF, Davoli MA *et al.* Single-nucleus transcriptomics of the prefrontal cortex in major depressive disorder implicates oligodendrocyte precursor cells and excitatory neurons. *Nat Neurosci* 2020; **23**: 771–781.

11 Perlman K, Couturier CP, Yaqubi M, Tanti A, Cui Q, Pernin F *et al.* Developmental trajectory of oligodendrocyte progenitor cells in the human brain revealed by single cell RNA sequencing. *Glia* 2020; **68**: 1291–1303.

12 Boulanger JJ, Messier C. Oligodendrocyte progenitor cells are paired with GABA neurons in the mouse dorsal cortex: Unbiased stereological analysis. *Neuroscience* 2017; **362**: 127–140.

13 Guadagno A, Verlezza S, Long H, Wong TP, Walker CD. It is all in the right amygdala: Increased synaptic plasticity and perineuronal nets in male, but not female, juvenile rat pups after exposure to early-life stress. *J Neurosci* 2020; **40**: 8276–8291.

14 Gildawie KR, Honeycutt JA, Brenhouse HC. Region-specific effects of maternal separation on perineuronal net and parvalbumin-expressing interneuron formation in male and female rats. *Neuroscience* 2019. doi:10.1016/j.neuroscience.2019.12.010.

15 Ueno H, Suemitsu S, Murakami S, Kitamura N, Wani K, Matsumoto Y *et al.* Juvenile stress induces behavioral change and affects perineuronal net formation in juvenile mice. *BMC Neurosci* 2018; **19**: 1–21.

16 Alcaide J, Guirado R, Crespo C, Blasco-Ibáñez JM, Varea E, Sanjuan J *et al.* Alterations of

perineuronal nets in the dorsolateral prefrontal cortex of neuropsychiatric patients. *Int J Bipolar Disord* 2019; **7**: 24.

17 Helmeke C, Ovtscharoff W, Poeggel G, Braun K. Imbalance of immunohistochemically characterized interneuron populations in the adolescent and adult rodent medial prefrontal cortex after repeated exposure to neonatal separation stress. *Neuroscience* 2008; **152**: 18–28.

18 Grassi-Oliveira R, Honeycutt JA, Holland FH, Ganguly P, Brenhouse HC. Cognitive impairment effects of early life stress in adolescents can be predicted with early biomarkers: Impacts of sex, experience, and cytokines. *Psychoneuroendocrinology* 2016; **71**: 19–30.

19 Uchida T, Furukawa T, Iwata S, Yanagawa Y, Fukuda A. Selective loss of parvalbumin-positive GABAergic interneurons in the cerebral cortex of maternally stressed Gad1-heterozygous mouse offspring. *Transl Psychiatry* 2014; **4**: e371.

20 Uchida T, Furukawa T, Yanagawa Y, Fukuda A. Maternal stress reduces parvalbumin positive GABAergic interneuron proliferation. *Dev Med Child Neurol* 2012.

21 Hu W, Zhang M, Czéh B, Flügge G, Zhang W. Stress impairs GABAergic network function in the hippocampus by activating nongenomic glucocorticoid receptors and affecting the integrity of the parvalbumin-expressing neuronal network. *Neuropsychopharmacology* 2010. doi:10.1038/npp.2010.31.

22 Holland FH, Ganguly P, Potter DN, Chartoff EH, Brenhouse HC. Early life stress disrupts social behavior and prefrontal cortex parvalbumin interneurons at an earlier time-point in females than in males. *Neurosci Lett* 2014; **566**: 131–6.

23 Heim C, Mletzko T, Purselle D, Musselman DL, Nemeroff CB. The Dexamethasone/Corticotropin-Releasing Factor Test in Men with Major Depression: Role of Childhood Trauma. *Biol Psychiatry* 2008; **63**: 398–405.

24 Devienne G, Picaud S, Cohen I, Piquet J, Tricoire L, Testa D *et al.* Regulation of perineuronal nets in the adult cortex by the electrical activity of parvalbumin interneurons. bioRxiv. 2019. doi:10.1101/671719.

25 Cisneros-Franco JM, De Villers-Sidani É. Reactivation of critical period plasticity in adult auditory cortex through chemogenetic silencing of parvalbumin-positive interneurons. *Proc Natl Acad Sci U S A* 2019. doi:10.1073/pnas.1913227117.

26 Deidda G, Allegra M, Cerri C, Naskar S, Bony G, Zunino G *et al.* Early depolarizing GABA controls critical-period plasticity in the rat visual cortex. *Nat Neurosci* 2015. doi:10.1038/nn.3890.

27 Heim C, Newport DJ, Mletzko T, Miller AH, Nemeroff CB. The link between childhood trauma and depression: Insights from HPA axis studies in humans. *Psychoneuroendocrinology* 2008; **33**: 693–710.

28 Huang ZJ, Kirkwood A, Pizzorusso T, Porciatti V, Morales B, Bear MF *et al.* BDNF regulates the maturation of inhibition and the critical period of plasticity in mouse visual cortex. *Cell* 1999. doi:10.1016/S0092-8674(00)81509-3.

29 Cirulli F, Francia N, Berry A, Aloe L, Alleva E, Suomi SJ. Early life stress as a risk factor for mental health: Role of neurotrophins from rodents to non-human primates. Neurosci. Biobehav. Rev. 2009. doi:10.1016/j.neubiorev.2008.09.001.

30 Begum MR, Sng JCG. Molecular mechanisms of experience-dependent maturation in cortical GABAergic inhibition. J. Neurochem. 2017. doi:10.1111/jnc.14103.

31 Beurdeley M, Spatazza J, Lee HHC, Sugiyama S, Bernard C, Di Nardo AA *et al.* Otx2 binding to

perineuronal nets persistently regulates plasticity in the mature visual cortex. *J Neurosci* 2012; **32**: 9429–37.

32 Peña CJ, Kronman HG, Walker DM, Cates HM, Bagot RC, Purushothaman I *et al.* Early life stress confers lifelong stress susceptibility in mice via ventral tegmental area OTX2. *Science (80-)* 2017. doi:10.1126/science.aan4491.

33 Kaufman J, Wymbs NF, Montalvo-Ortiz JL, Orr C, Albaugh MD, Althoff R *et al.* Methylation in OTX2 and related genes, maltreatment, and depression in children. *Neuropsychopharmacology* 2018. doi:10.1038/s41386-018-0157-y.

34 Dityatev A, Brückner G, Dityateva G, Grosche J, Kleene R, Schachner M. Activity-dependent formation and functions of chondroitin sulfate-rich extracellular matrix of perineuronal nets. *Dev Neurobiol* 2007; **67**: 570–588.

35 Simard S, Coppola G, Rudyk CA, Hayley S, McQuaid RJ, Salmaso N. Profiling changes in cortical astroglial cells following chronic stress. *Neuropsychopharmacology* 2018. doi:10.1038/s41386-018-0105-x.

36 Song I, Dityatev A. Crosstalk between glia, extracellular matrix and neurons. Brain Res. Bull. 2018. doi:10.1016/j.brainresbull.2017.03.003.

37 Carulli D, Rhodes KE, Brown DJ, Bonnert TP, Pollack SJ, Oliver K *et al.* Composition of perineuronal nets in the adult rat cerebellum and the cellular origin of their components. *J Comp Neurol* 2006; **494**: 559–577.

38 Velmeshev D, Schirmer L, Jung D, Haeussler M, Perez Y, Mayer S *et al.* Single-cell genomics identifies cell type–specific molecular changes in autism. *Science (80-)* 2019; **364**: 685–689.

39 Kumar MP, Du J, Lagoudas G, Jiao Y, Sawyer A, Drummond DC *et al.* Analysis of Single-Cell RNA-Seq Identifies Cell-Cell Communication Associated with Tumor Characteristics. *Cell Rep* 2018; **25**: 1458-1468.e4.

40 Habib N, Avraham-Davidi I, Basu A, Burks T, Shekhar K, Hofree M *et al.* Massively parallel single-nucleus RNA-seq with DroNc-seq. *Nat Methods* 2017. doi:10.1038/nmeth.4407.

41 Yang SM, Michel K, Jokhi V, Nedivi E, Arlotta P. Neuron class–specific responses govern adaptive myelin remodeling in the neocortex. *Science (80-)* 2020; **370**. doi:10.1126/SCIENCE.ABD2109.

42 Orduz D, Benamer N, Ortolani D, Coppola E, Vigier L, Pierani A *et al.* Developmental cell death regulates lineage-related interneuron-oligodendroglia functional clusters and oligodendrocyte homeostasis. *Nat Commun* 2019; **10**: 4249.

43 Orduz D, Maldonado PP, Balia M, Vélez-Fort M, de Sars V, Yanagawa Y *et al.* Interneurons and oligodendrocyte progenitors form a structured synaptic network in the developing neocortex. *Elife* 2015; **2015**: 1–53.

44 Lin SC, Bergles DE. Synaptic signaling between GABAergic interneurons and oligodendrocyte precursor cells in the hippocampus. *Nat Neurosci* 2004. doi:10.1038/nn1162.

45 Vélez-Fort M, Maldonado PP, Butt AM, Audinat E, Angulo MC. Postnatal switch from synaptic to extrasynaptic transmission between interneurons and NG2 cells. *J Neurosci* 2010. doi:10.1523/JNEUROSCI.0238-10.2010.

46 Lutz P-E, Tanti A, Gasecka A, Barnett-Burns S, Kim JJ, Zhou Y *et al.* Association of a History of Child Abuse With Impaired Myelination in the Anterior Cingulate Cortex: Convergent Epigenetic, Transcriptional, and Morphological Evidence. *Am J Psychiatry* 2017; : appiajp201716111286.

47 Tanti A, Kim JJ, Wakid M, Davoli M-A, Turecki G, Mechawar N. Child abuse associates with an imbalance of oligodendrocyte-lineage cells in ventromedial prefrontal white matter. *Mol Psychiatry* 2018; **23**: 2018–2028.

48 Wellman CL, Bangasser DA, Bollinger JL, Coutellier L, Logrip ML, Moench KM *et al.* Sex Differences in Risk and Resilience: Stress Effects on the Neural Substrates of Emotion and Motivation. *J Neurosci* 2018; **38**: 9423–9432.

49 Gildawie KR, Honeycutt JA, Brenhouse HC. Region-specific Effects of Maternal Separation on Perineuronal Net and Parvalbumin-expressing Interneuron Formation in Male and Female Rats. *Neuroscience* 2020. doi:10.1016/j.neuroscience.2019.12.010.

Table 1. Subjects characteristics

	CTRL	DS-CA	DS
N	11	12	16
Axis 1 diagnosis	0	MDD (11); DD-NOS (1)	MDD (14); DD-NOS (2)
Age (years)	43.18 ± 7.11	37.75 ± 3.10	46.63 ± 3.48
Sex (M/F)	9/2	9/3	14/2
PMI (hours)	35.95 ± 7.15	40.92 ± 6.68	45.95 ± 8.06
Tissue pH	6.4 ± 0.09	6.56 ± 0.08	6.52 ± 0.07
Substance dependence	0	5	6
Medication	0	SSRI (2); Benzodiazepines (2); Antipsychotics (1); Antimanic (1)	SSRI (4); SNRI (1); TCA antidepresants (1); Benzodiazepines (3); Antipsychotics (2); Antimanic (1)

Data represent mean ± s.e.m. PMI: Post-mortem interval; MDD: Major Depressive Disorder; DD-NOS: Depressive Disorder Not Otherwise Specified. SSRI: Selective Serotonin Reuptake Inhibitor; SNRI: Selective Norepinephrine Reuptake Inhibitor; TCA: tricyclic antidepressant.

Figure Legends

Figure 1. (**A**) Representative images of PNNs labeled with WFL and their distribution throughout the cortical layers of the human vmPFC. Scale bars = 100 and 20 µm (high magnification panel) (**B**) Depressed suicides with a history of child abuse (DS-CA, N = 11) have significantly higher densities of PNNs compared to controls (CTRL, N = 10) and depressed suicides without history of child abuse (DS, N= 14) (layer x group: $F(10, 115) = 2.07$, $P< 0.05$). (**C**) Representative images of in situ hybridization for PVALB (green) followed by WFL labeling (red). Nuclei were stained with DAPI (cyan). Yellow arrowhead points to a PVALB+/PNN- cell. Scale bars = 25µm. (**D**) DS-CA (N=9) subjects have higher ratios of PVALB+ cells surrounded by PNNs compared to CTRLs (N =8) and DS subjects (N=4) (Kruskal-Wallis ANOVA $H(2,21) = 9.45$, $P<0.01$). (**E**) Representative images of a low (top) and high (bottom) intensity PNN in the vmPFC. (**F**) PNNs from DS-CA subjects (N=475; 6) showed higher average WFL intensity compared to CTRLs (N= 387; 6) or DS (N=479; 5) (One-way ANOVA: $F(2, 1338) = 80.56$, $P<0.001$) (**G**) PNNs from DS-CA subjects (N=432; 6) showed

higher complexity (area covered by PNNs) compared to CTRLs (N= 363; 6) or DS (N=467; 5) (One-way ANOVA: F (2, 1259) = 11.06, P<0.001). Tukey's multiple comparison test or Dunn's test: ***:P<0.001, **: P<0.01, *:P<0.05, #:P<0.1.

Figure 2. (A) Expression of canonical components of PNNs according to cell type, derived from single-nucleus RNA sequencing of 34 human PFC samples (11). OPCs consistently express higher levels of most of these components compared to other cell types. (**B**) Representative images of FISH validation of VCAN (Versican, yellow) expression in OPCs (PDGFRA+ cells, white). Note the VCAN expressing OPC juxtaposed to a PVALB+ (magenta) cell. Nuclei were counterstained with DAPI (blue). Scale bar = 5 µm. (**C**) Representative images of FISH validation of PTPRZ1 (Phosphacan, yellow) expression in OPCs (PDGFRA+ cells, white). Nuclei were counterstained with DAPI (blue). Scale bar = 5 µm. (**D-E**) Both VCAN (**D**) and PTPRZ1 (**E**) expression is highly enriched in OPCs, with 97.8 percent of VCAN+ cells (N=225) co-expressing PDGFRA (**D**), and 91.8 percent of PTPRZ1+ cells (N= 281) co-expressing PDGFRA (**E**). (**F**) A negative correlation was found between average distance of OPCs from closest PVALB+ cell and PNNs density (R^2 = 0.36, P<0.05), suggesting that OPCs proximity with PVALB+ cells could reflect changes in PNN density. (**G**) Proximity of OPCs with PVALB+ cells was increased in DS-CA subjects (N=90 OPCs, 5 subjects) compared to CTRLs (N= 106 OPCs, 6 subjects) and DS (N= 73 OPCs, 4 subjects) (One-way ANOVA: F (2, 266) = 7.963, P<0.001). (**H-I**) Both PTPRZ1 (**H**) and TNR (**I**) average expression in OPCs modestly correlated with PNNs densities (R^2 = 0.35, P<0.05 and R^2 = 0.28, P<0.05 respectively). (**J**) The average expression of VCAN in OPCs was significantly higher in DS-CA subjects (N=139 cells, 7 subjects) compared to CTRLs (N= 160 cells, 8 subjects) and DS (N= 119 cells, 6 subjects) (One-way ANOVA F (2, 415) = 17.25, P<0.001). (**K**) The average expression of PTPRZ1 in OPCs was significantly higher in DS-CA subjects (N=63 cells, 4 subjects) compared to CTRLs (N= 117 cells, 6 subjects) and DS (N= 81 cells, 5 subjects) (One-way ANOVA F (2, 258) = 31.65, P<0.001). (**L**) The average expression of TNR in OPCs was significantly higher in DS-CA subjects (N=200 cells, 8 subjects) compared to CTRLs (N= 207 cells, 7 subjects) and DS (N= 160 cells, 5 subjects) (One-way ANOVA, F (2, 564) = 18.69, P<0.001). Tukey's multiple comparison test: ***:P<0.001, *:P<0.05.

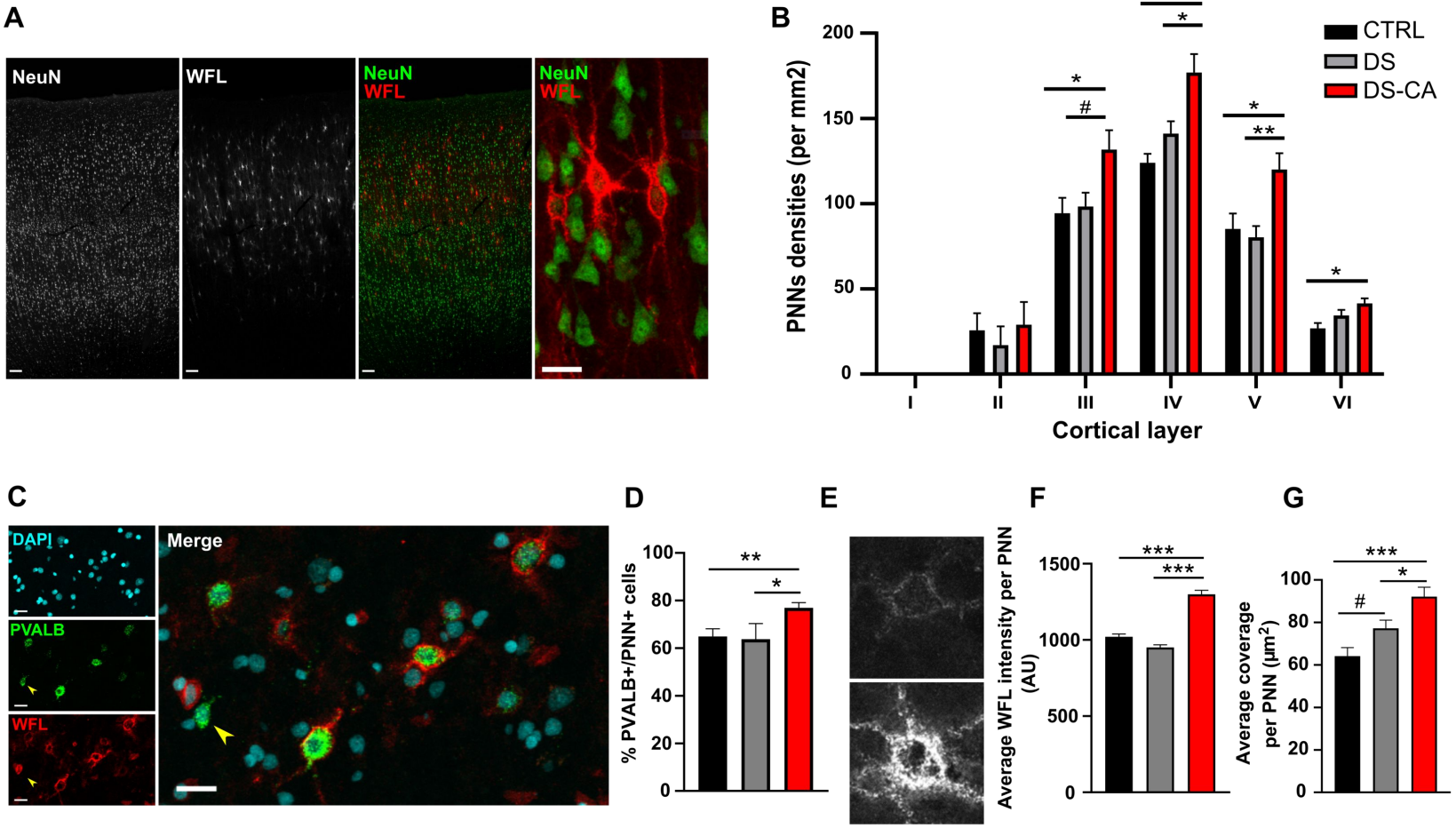
A
NeuN
WFL
NeuN
WFL
NeuN
WFL
B
CTRL
DS
DS-CA
PNNs densities (per mm2)
200
150
100
50
0
I
II
III
IV
V
VI
Cortical layer
C
DAPI
PVALB
WFL
Merge
D
% PVALB+/PNN+ cells
100
80
60
40
20
0
E
F
Average WFL intensity per PNN (AU)
1500
1000
500
0
G
Average coverage per PNN (µm²)
100
80
60
40
20
0

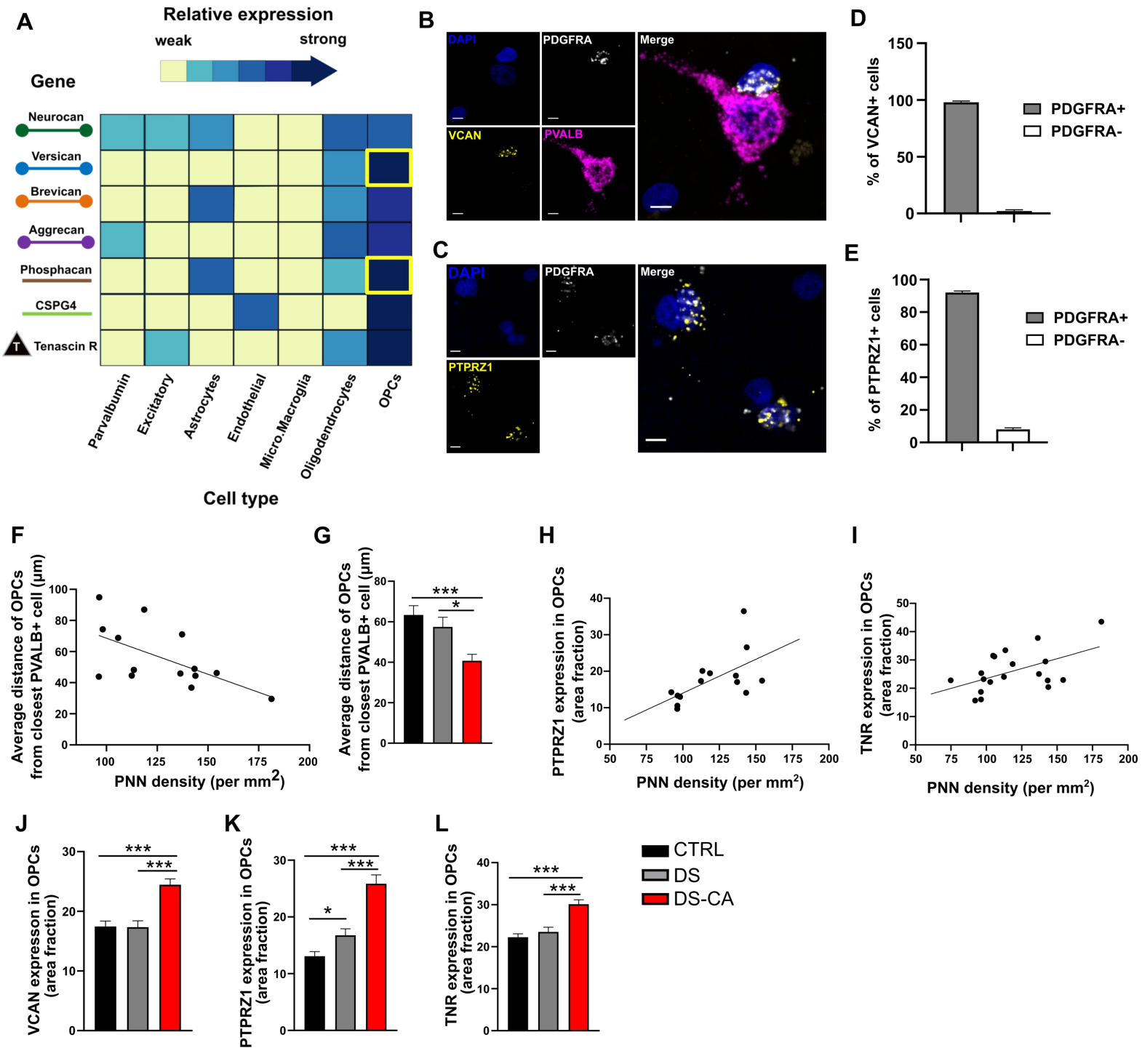
A
Relative expression
weak
strong
Gene
Neurocan
Versican
Brevican
Aggrecan
Phosphacan
CSPG4
Tenascin R
Parvalbumin
Excitatory
Astrocytes
Endothelial
Micro.Macroglia
Oligodendrocytes
OPCs
Cell type
B
DAPI
PDGFRA
Merge
VCAN
PVALB
C
DAPI
PDGFRA
Merge
PTPRZ1
D
% of VCAN+ cells
PDGFRA+
PDGFRA-
E
% of PTPRZ1+ cells
PDGFRA+
PDGFRA-
F
Average distance of OPCs from closest PVALB+ cell (µm)
PNN density (per mm2)
G
Average distance of OPCs from closest PVALB+ cell (µm)
H
PTPRZ1 expression in OPCs (area fraction)
PNN density (per mm2)
I
TNR expression in OPCs (area fraction)
PNN density (per mm2)
J
VCAN expresson in OPCs (area fraction)
K
PTPRZ1 expression in OPCs (area fraction)
L
TNR expression in OPCs (area fraction)
CTRL
DS
DS-CA